LUT University
LUT School of Energy Systems
LUT Mechanical Engineering

Matti Heinonen

THE RELATIONSHIP BETWEEN ATTENUATION AND THERMAL PROFILE IN DRAW PROCESS OF A SINGLE-MODE GE-DOPED OPTICAL FIBER

Updated 15.6.2020

Examiners: Professor Juha Varis
M.Sc. Risto Widerholm

TIIVISTELMÄ

LUT-Yliopisto
LUT School of energy systems
LUT Kone

Matti Heinonen

THE RELATIONSHIP BETWEEN ATTENUATION AND THERMAL PROFILE IN DRAW PROCESS OF A SINGLE-MODE GE-DOPED OPTICAL FIBER

Diplomityö

2020

58 sivua, 13 kuvaa ja 40 taulukkoa

Tarkastajat: Professor Juha Varis
M.Sc. Risto Widerholm

Hakusanat:

Tämän diplomityön tavoitteena on on tutkija valokuidun valmistuksesa käytettävän uunin jatkoputken merkitystä tuotteen laatuun. Avaintekijänä on lämpötilamuutoksen ja kuidusta mitatun vaimennuksen välisen suhteen selvittäminen. Mittaaminen suoritettiin Rosendahl Nextrom Oy:n toimitiloissa Vantaalla. Työssä mitataan kuidun lämpötilaa SIKORA mittalaitteella ja kuidun vaimennusta analysoidaan Photon Kinetics mittalaitteilla. Tulosten käsittelyä varten on mitattujen lämpötilojen perusteella laskettu lämmönmuutosnopeus *(°C/s)*, jota verrataan saatuihin valokuidun vaimennusarvoihin. Muodostunut data on sen jälkeen tarkasteltu muuttujien, kuten käytetyn lasipreformin, vaikutusten selvittämiseksi.

Lopputuloksena työssä kerätyn datan voidaan sanoa olleen riittämätön laajuudessaan. Toinen merkittävä muuttuja, jonka vaikutukset olivat merkittäviä lopputuloksen kannalta, oli käytettyjen lasipreformien lyhyt pituus ja vaihteleva laatu. Tarkastelu viittaa lämmönmuutosnopeuden ja vaimennuksen olevan kääntäen verrannollinen, mutta ilman laajempaa näytemäärää ei mitään ennustavaa yhtälöä voida muodostaa.

ABSTRACT

LUT University
LUT School of energy systems
LUT Mechanical Engineering

Matti Heinonen

THE RELATIONSHIP BETWEEN ATTENUATION AND THERMAL PROFILE IN DRAW PROCESS OF A SINGLE-MODE GE-DOPED OPTICAL FIBER

Master's thesis

2020

58 pages, 13 Figures and 40 Tables

Examiners: Professor Juha Varis
M.Sc. Risto Widerholm

Keywords:

The objective of this thesis is to measure the relationship between attenuation and the thermal profile of a single-mode optical fiber. Measuring was executed by drawing fiber at Rosendahl Nextrom Oy, Vantaa facility and recording the thermal values of the fiber from several different positions. Photon Kinetics instruments were used to measure attenuation in produced fiber samples. The analysis was performed by comparing calculated cooling rate values *(°C/s)* to the achieved attenuation Figures.

The formed data was carefully analyzed for outliers from undesirable influencers like inconsistent preform quality. As a conclusion the data collected suggests that the rate of cooling the fiber experiences is inversely related to the measured attenuation. However, data set can not be held reliable due to smaller than intended amount of draws and the unforeseen variations in attenuation that could be a result of the unideal selection of used preforms. As a consequence of the factors mentioned, any predictive formula could not be made.

ACKNOWLEDGEMENTS

The operation of the process for all the draws done for the thesis, the learning that has taken three years and the invaluable insight to inner workings of a draw tower are all owed to the senior process engineers working with OFC 20 draw tower. Special thanks to Joonas, Urmas, Manu, Heikki, Risto and Sylvain who have been essential to my development of understanding with the draw tower.

Matti Heinonen

Matti Heinonen
Helsinki 14.6.2020

Table of Contents

LIST OF SYMBOLS AND ABBREVIATIONS

FCS	Fiber Cooling System
Fiber	Shortened form of the silica-glass optical fiber used in the trials of this research. This fiber has a germanium doped core and is designed as a single-mode signal transmission medium.
FOC	Fiber Optic Center
ID	Inside diameter
IEEE	Institute of Electrical and Electronics Engineers
ITU	International Telecommunication Union
NIF	Nextrom Induction Furnace
NPF	Nextrom Preform Feeding
OD	Outside diameter
R&D	Research and development
Tf	Fictive temperature
Tg	Glass transition temperature
ΔT	Cooling rate [$°C/s$]

1 INTRODUCTION

Rosendahl Nextrom Oy manufactures production equipment for international customer base and its Vantaa based branch, which is the Nextrom, specializes in optical fiber and cable production machinery. Nextrom equipment spans from the creation of the glass preforms all the way to the final cable machines that create the final in-use product. This research concentrates solely on the fiber draw process of the telecommunications grade silica-based optical fiber that has a germanium doped core. Part of the benefit, in business sense, for Nextrom is obviously knowing the best setup for its equipment. This will add to the success that their customers can achieve in production. Therefore, a large part of the process of negotiation and planning with customers will be the interconnected nature of factory lay-out, equipment setup and agreed acceptance criteria.

Conventional wisdom dictates that the optical fiber must have enough time to cool below its fictive temperature (*Tf*) before it is exposed to cool room air that will accelerate the cool down. This is why drawing speed and extension tube length are two dynamic factors that need to be considered. As the production speed increases, the time in which the fiber must reach *Tf* reduces. This means that the extension tube must be longer to allow for longer controlled cooling period.

Previous experience in the field shows us how the rate of cooldown of the fiber from process temperatures affects the built-up tensions inside the glass fiber. These tensions affect the refractive index and in turn increase the amount of signal loss, known as attenuation, in the optical fiber. The ability to control and predict what effect certain changes in the draw process have in final attenuation level of the fiber will pave the way towards more efficient production. It is still important to remember that a single parameter alone will not enable a great leap forward, but rather is one step in the progress that happens with incremental advancements in each limiting area of the process.

1.1 Research problem, goal and boundaries

Knowing the recommended length of the extension tube can be hard to quantify and present in numbers accurately with the current draw speeds. As the technology for optical fiber progresses and the speed at which the fiber is drawn increases, so do increase the demands that it sets on each component of the drawing process. Previously existed standard lengths of the extension tube might prove insufficient at some point as the drawing speed increases. During field commissioning of the Rosendahl Nextrom machinery some clues have been experienced that could point towards the possibility of design optimization. Therefore, the problem is to quantify the necessary length needed for the expected quality and learning how a short tube will be affecting the commonly measured values in the optical fiber. Furthermore, hopefully some threshold length could be determined between having a sufficient cooling rate and point of diminishing returns in length for fiber quality.

Goal of this paper is to add some empirical testing to the existing knowledge, and then see what effects can be found in the quality markers of the produced optical fiber. This target is to map out quantitatively how the cooling rate of the optical fiber affects the attenuation, or signal loss, in a single-mode optical fiber. The focus will be put on researching how the thermal profile will be affected by changes to the length of exposed fiber between the furnace and cooling tubes. As the fiber exits the furnace extension tube at high temperature it experiences rapid cooling. The routinely measured cold fiber temperature can be used to determine the amount of cooling needed, but the rate of cooling prior to cooling tubes is often overlooked.

In practical terms the analysis of the cooling rate aims to see how the critical area of exposed hot fiber from the furnace extension tube until the fiber cooling system (FCS), will affect the attenuation in finished optical fiber. Problems rise when trying to determine which factor is the root cause for the change in measured values. This is why the validity of results will be determined by the quantity of tests within each set of variables. Changes in preforms themselves can influence the results greatly. Cutoff can change from preform to preform and therefore affect the fictive temperature, which would affect the attenuation in the fiber. To add to the complexity, the Fiber Optic Center (FOC) in the Nextrom premises in Vantaa is centered around a large variety of R&D based draws, which introduces changes to the

process. During the research new preform manufacturing was under testing and the quality of the made preform cannot be described to be stable. Therefore, foreign quality preforms from reputable manufacturer must be used for control. There is no stable continuous optical fiber production in Vantaa to take advantage of for the purposes of this study. This all means that the amount of data collected needs to be extensive in order to mitigate the effect of outliers on the main body of data.

1.2 Single-mode optical fiber

When transmitting information, the single-mode optical fibers are the common workhorse for data transfer. It is the most efficient way of achieving dependable, fast, low loss and high bandwidth communication over long distances. Optical fibers function by transmitting pulses of light, which are then interpreted as binary information. (Neumann 1988, p. 9; Mitschke 2016, p. 9)

Single mode fiber, as the name implies, has only one mode of transmission. The core of the fiber is small unlike in multimode fibers, as can be seen demonstrated below (Figure 1). Single-mode fibers are excellent in terms of having low distortion due to the small core size and the singular light-wave. Compared to multimode fibers, single-mode fibers have higher bandwidth, work better for longer distance and higher transmission rate. Due to differences in performance along the attenuation spectrum, the typically used wavelengths are 1310 and 1550 nanometers which have lower loss. This is due to the loss peak, which dictates these two wavelengths to be beneficial in terms of low attenuation. (Fiber Onda 2017)

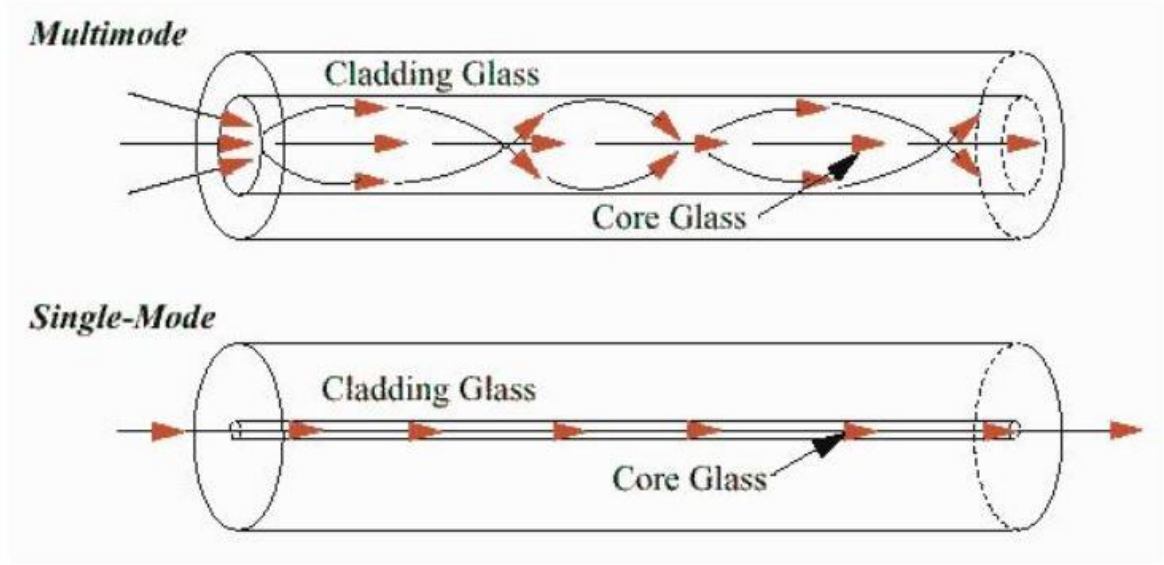

Figure 1. Visualization of differences on light inside the optical core between single-mode and multi-mode fibers. (Fiber Onda 2017)

Structure of the fiber consists of coating, cladding and core. Coating is typically in two parts, inside fluid primary resin and a UV hardened outer layer that gives the otherwise fragile glass fiber its strength. Standard single-mode optical fibers have an outer diameter of 245 µm (Figure 2). The cladding has an outside diameter of 125 µm and acts as a boundary to the core, as it has a different refractive index. The homogenous core, which is the medium that carries the signal, is itself about eight to ten micrometers in diameter and is usually doped. The dopant can vary but the most widely used element in telecommunication single-mode fibers is germanium. Therefore, these fibers are referred to as Ge-doped silica-based single-mode optical glass-fibers. (Neumann 1988, p. 12-15; Mitschke 2016, p. 17-19; Fiber Onda, 2017)

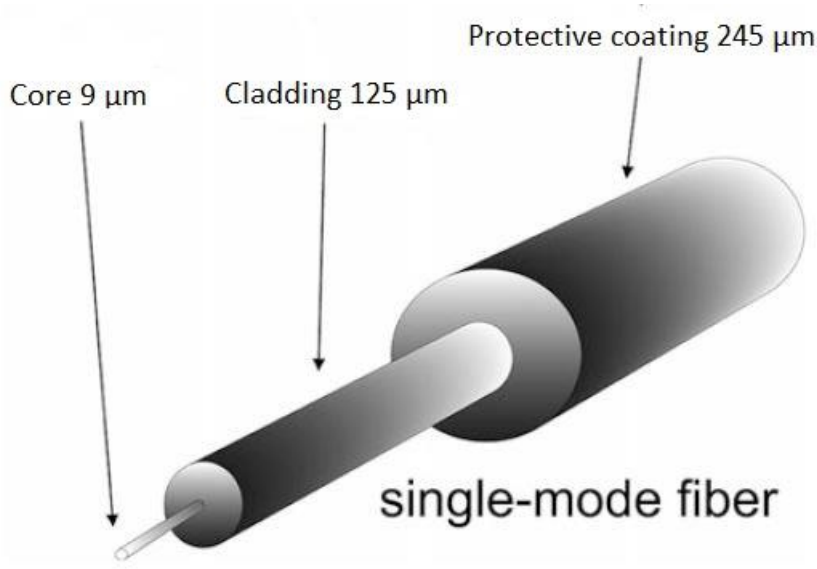

Figure 2. Representation of single-mode fiber structure (modified Mitschke 2016, p. 8)

The transfer of signal inside the core of a fiber is base on total internal reflection. At a low enough angle light is completely reflected in the boundary between 2 materials with different refractive indexes. Maximum angle for total internal reflection is defined by the refractive indexes of the core and the cladding. Therefore, some special applications have more exotic doping elements are needed to create a core that is capable of sufficient signal transfer efficiency despite smaller radius bends in the cable. (Neumann 1988, p. 14-15; Mitschke 2016, p. 17)

1.3 Silicate glass

Fiber optic cables that are made for telecommunications networks commonly utilize silica-based glass. Ter-Mikirtychev writes: “Silica-based fibers have several advantages over other glass types used in fiber manufacturing.” He continues to emphasize the key role of easy manufacturability that allows for longer lengths of fiber to be produced. Telecommunication fiber production is a high-volume business and as such the uninterrupted production and high yield are important for final price per kilometer. With the germanium doped cores, the larger preforms for telecom-fibers are even 8 meters long and 200 mm in diameter. Such high volume preforms take very long to draw. At a feed rate of 1.0 ± 0.1 mm/min and a preform length of 8000 mm, a continuous and uninterrupted draw takes over 133 hours to

finish. Another strength of silicate glass is also its optical clarity. This low loss is good for long distance communication and lowers the numbers of necessary intermediate stations to boost the signal. Silicate glass fibers are also very tolerant to bending and handle mechanical stresses well, as well as being very resistive to water and chemicals. (Ter-Mikirtychev 2014, p. 33)

1.4 Attenuation

The loss of power over a transferring medium, here optical fiber, is referred to as attenuation. It is measured as decibels per kilometer (dB/km) is one of the essential quality characteristics of long-distance telecommunications fibers. The current record for how low attenuation one can get stands at 0.1419 dB/km, which was measured at 1560 nm wavelength. This record was published in 2017 Optical Fiber Communications Conference and Exhibition according to IEEE. Fiber used for the record was a silica-core fiber with low 1290 degrees Celsius fictive temperature (chapter 2.2). (Neumann 1988, p. 104; IEEE 2017)

Attenuation has two (2) main wavelengths which are the common points of reference that are stated in standards as the minimum level that the fiber must achieve to pass for a fiber of that given standard or customer specification. These typical measurement wavelengths are 1310 and 1550 nanometers. For example, the ITU-T standard G.654 dictates a level of below 0.22 dB/km must be achieved for qualification. The reason for these specific wavelengths can be seen in Figure 3. At these wavelengths the loss of dB/km is the lowest on either side of the peak caused by absorption of impurities in the glass. As seen in Figure 3, the curves of Rayleigh scattering and the natural Infrared absorption both favor the higher wavelength of 1550 nm. Attenuation value for the 1310 nm is naturally higher in comparison due to being higher up the Rayleigh scattering slope. In the literature and industry this higher 1550 nm wavelength is frequently not specified but assumed when the value of attenuation is advertised or stated for optical fibers. (ITU-T G.654 2016; Mitschke 2016, p. 88)

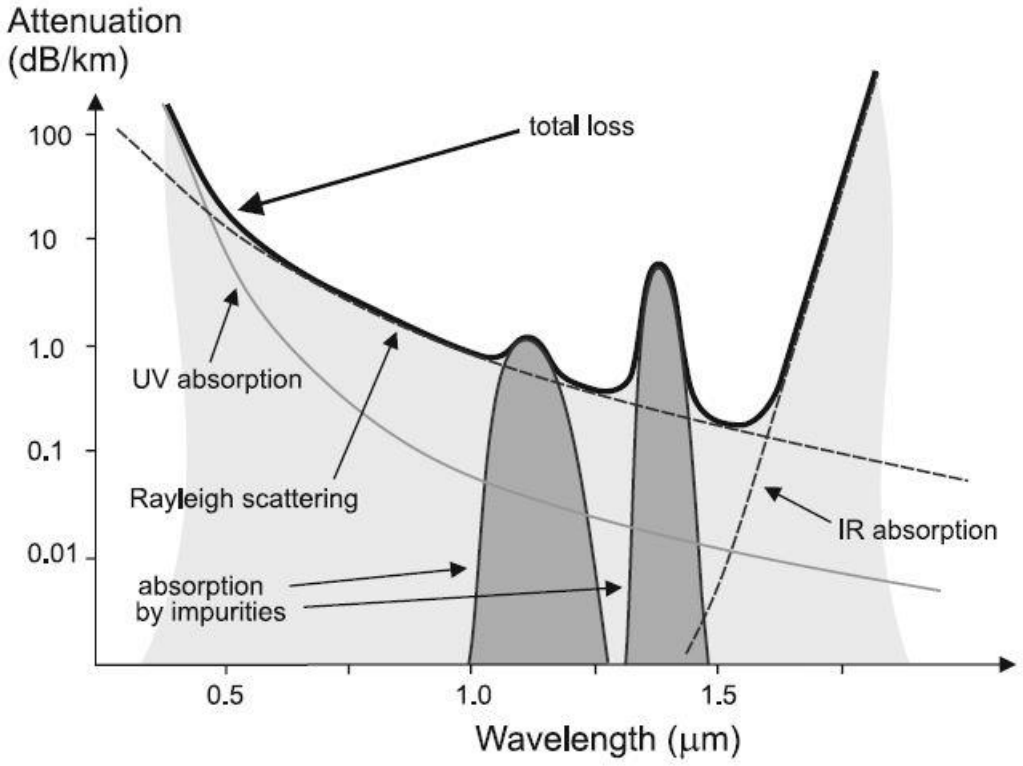

Figure 3. Spectrum of attenuation in relation to wavelength. Notice the low point roughly at 1.3 and 1.5 μm (Mitschke 2016, p. 88)

Values below 0.2 dB/km are achieved routinely as quality for typical single-mode fiber. Typical in this case would be conforming with International Telecommunication Union (ITU) standards of G.652 and G.654. Simply because the distances covered by these common fibers is so great, any tenth, one hundredth of a dB/km matters greatly and can save millions of dollars depending on the scale of use. Mitschke wrote: "On any long-haul distance, a number of intermediate amplifiers or signal conditioners is required; their number can be reduced as soon as the loss goes down". This is why attenuation matters so much in single-mode applications, as the rewards are direct savings. (Mitschke, 2016, p. 88; ITU-T standard G.654 2016; ITU-T standard G.652 2009)

Relationship between attenuation and the cooling down of class is not new knowledge. The magnitude of the effect that fiber cooling has on attenuation was studied by Volotinen et al. in a 2003 publication with the title "Impact of Silica Glass Structure on Transmittance". In their study Volotinen et al. concluded that the transmittance, in other words attenuation, was

affected by the fictive temperature as well as residual tensions in the glass structure. These findings are based on Rayleigh Scattering (Chapter 1.4.1) phenomenon in which the density and concentrations fluctuations in the glass will affect the attenuation of the fiber. (Volotinen et al. 2003, p. 11-12)

1.4.1 Loss mechanisms

There are many ways in which the strength of a signal can get weaker. The end result from all of them is the same loss of performance. Any increase to attenuation is undesirable and is to be avoided. Next, we will introduce the more essential ways that attenuation can happen, from the perspective of this research. Certain mechanisms, like microbending loss, transition loss, Raman scattering and stimulated Brillouin-scattering are not explained but can be found in the same sources.

Rayleigh scattering is an intrinsic loss mechanism that dictates how low the attenuation can possibly be. This phenomenon is not only specific to optical fibers or transmittance in any type of glass but applies to all transparent materials that are not perfectly homogenous. As was shown before in Figure 3, the use of higher wavelengths decreases the amount of scattering. Originally John William Strutt, also known as Lord Rayleigh, determined the blue of the sky to be a result of bright light scattering from atmospheric particles. In this example the longer wavelengths of yellow to red during sunsets and sunrises are scattered less and those rays of light experience a lower angle of scattering. Same phenomenon takes place inside a glass fiber because of its fluctuations in density and concentration. During manufacturing the glass fiber solidifies quickly from a molten state and so freezes these fluctuations in place. (Neumann 1988, p. 109; Mitschke 2016, p. 87-89)

Intrinsic absorption creates a buildup of heat in glass fibers. Unlike scattering, the energy of the travelling photons is not redirected but absorbed into the medium. Absorption happens when the photons travelling through excite the electrons bound in the glass structure. Decreasing wavelength below 700 nm increases attenuation by absorption greatly and as a result there is a concept of UV-absorption edge (Figure 3). On the other side of the spectrum with wavelengths exceeding 1600 nm the attenuation increases very rapidly with the IR-

absorption edge (Figure 3). Common germanium doping in the core of an optical fiber slightly increases the loss from intrinsic absorption. (Neumann 1988, p. 111-112)

Impurity absorption specifies the losses in attenuation as a result of impurities like water, transitional metals, hydroxyls- and hydrogen ions. Transition metals like iron, copper, cobalt, chrome, nickel and manganese cause large increase in attenuation even in small concentrations. For reference Mitschke wrote: "At 800 nm, one part per billion of Cu produces an absorption of several tenths of dB/km". However, modern preform fabrication uses sophisticated distillation and vapor deposition of chemicals to achieve extremely high levels of purity. This in effect then results in losses from transitional metals to be at negligible levels. Hydroxyl ion (OH^-) contamination causes attenuation peaks at 1390, 1250 and 950 nm wavelengths. The attenuation peak of 1390 nm is in between the 1310 nm and 1550 nm low-loss windows (Figure 3). Because the size of this peak at 1390 nm will affect the values measured at 1310 and 1550 nanometers, it can be used for fiber quality estimation. (Neumann 1988, p.112; Mitschke 2016, p. 89)

Macro-bending is defined as the "macroscopic" bends of a fiber that are normally quantified in centimeters of radius. In a bent fiber the inside curvature of the fiber is under compression as on the opposite side of the fibers central axis the outside curve is being stretched. On the outside of the curvature the stretching of the glass lowers density which lowers the refractive index. This effectively decreases the difference between the refractive indexes of the clad and core. Additionally, the photons travelling the outer curvature can approach their maximum travel velocity, which will cause a loss as the photons start to radiate away. The loss from a bend increases as the signal will penetrate the cladding exponentially, as the bend radius gets smaller. (Neumann 1988, p. 118; Mitschke 2016, p. 89)

1.5 Fictive temperature

Viscosity in glass increases rapidly as it cools down. This is in contrast with normal liquid-to-solid state transition. Furthermore, silica glass does not behave like a normal soda-lime glass. As seen in Figure 4 the volume of silica glass changes in a non-linear way as the temperature changes. However, for both glass types the cooling rate determines how little

time the internal structure has to change before it is frozen. Lancry et al. writes that “Fictive temperature (*Tf*) is the temperature at which the glass structure is frozen. It describes thus the structure of a glass and is related to the cooling rate”. This means that faster cooling rate results in a higher *Tf*. Comparing the Figures 4(a) and 4(b) shows how the the volume for Silica glass will stay lower compared to normal glass, when it has experienced a fast cooldown. (Lancry et al. 2012, p. 66-67)

Fictive temperature is used as a marker to define the structural state inside the glass but cannot be used to describe it accurately. Two different samples of glass fiber could be manipulated to have the same *Tf* without having the same internal structure. One can simply perform a continuous cool rate for one sample to achieve a *Tf* of 530 Celsius, and then hold the second sample at that 530 degrees until in equilibrium before cooling it rapidly. This has been called “the memory effect”. (Lancry et al. 2012, p. 66-67)

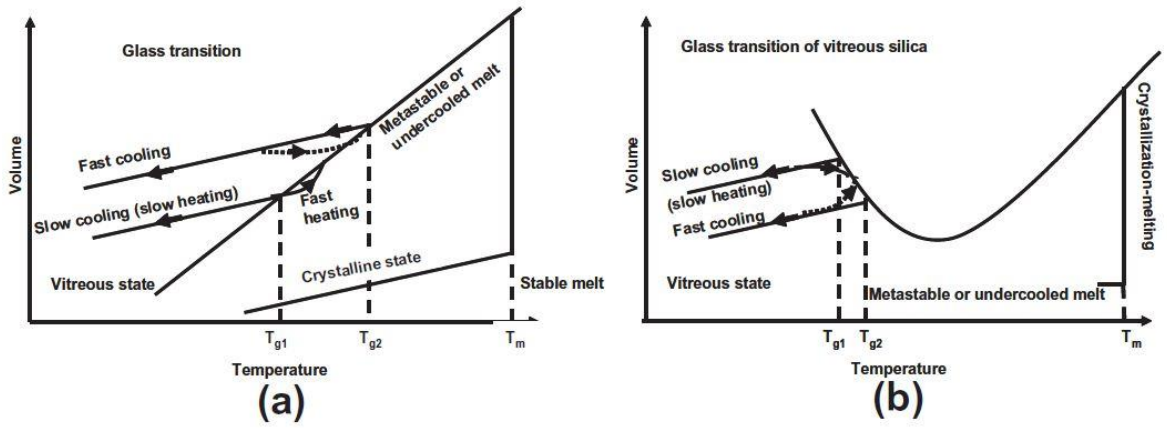

Figure 4. Graphic comparison of temperature-volumetric relationships in two different glass types. The graph (a) represents normal soda-lime glass and the graph (b) pure silica glass. (Lancry et al. 2012, p. 65)

Fibers thermal history determines what type of structures and therefore properties the silica glass will exhibit. These frozen structures will affect the type of intrinsic scattering that takes place due to the structures determined by cooling rate during the fiber draw process. Properties affected by thermal history include density, refractive index, hardness and mechanical strength and chemical durability. For the goal of this research the changes in refractive index and its effect on the intrinsic scattering are key components that need to be

understood in order to understand the basis for the research methodology. (Lancry et al. 2012, p. 67)

2 DRAWING PROCESS

Optical single-mode fiber is produced in a vertical draw tower. The height of this tower is dependent on the final product and drawing speed. As the drawing speed increases, so does the rate at which the fiber is needed to be cooled down. For context production speeds of 2500 meters per minute (m/min) require additional cooling systems to aid cooling and cannot rely on natural thermal transfer with the room air, while at 1500 m/min this could be unnecessary depending on the process and materials used. The optical fiber is drawn from a silica-glass preforms that are fed into a furnace vertically. In single-mode fiber the most common and cost-effective way to separate the refractive indexes of the glass core and cladding is to dope the core with germanium. At current date the common size of the preform is 150 mm in diameter and from two to eight meters long.

The method of production for telecommunication fiber optics is meant to provide a linear and controlled “pulling” or “drawing” of the fiber from the melt at the tip of the preform. Melt position is determined in the process lingo as the center of the coil. However, in reality this is not the only point where the glass is molten. The tip of the preform is elongated by the drawing and the faster the process speed is the longer the neck of the preform will stretch. Final outside diameter of the glass fiber without the acrylate coating is 125 µm when talking of single-mode telecommunication fiber. This final diameter is routinely only reached inside the upper part of extension tube or lower parts of the furnace. The exact location is dependent on the drawing speed. At the speed of 2500 m/min, which is 41.7 meters per second (m/s), the fiber spends a very short time inside the extension tube before exiting to the relatively cold room air.

Due to the requirements on the quality of the fiber optics, the draw towers need to be aligned perfectly vertical and this is often refined to a high degree. The variation on X or Y -plane between top and bottom of the tower (Figure 5) should be 0-2 millimeters at maximum and constant care for alignment is common to perfect their relative positions to one another. The overall height of a tower is largely determined by its targeted process speed. Faster drawing speeds need longer intervals between tower components. In higher drawing speeds, like 2500

m/min, for correct cooling of the fiber to happen the time inside the cooling tubes needs to be adequate for sufficient heat transfer with the cooled helium gas. Also, the coating that is fed over the glass fiber needs enough time within the UV curing lamps, so that the secondary acrylate coating cures completely. Fully cured secondary coating, that forms the top layer of the final fiber, is essential for the mechanical strength of the produced optical fiber. Without the primary and secondary acrylate coating the fiber is very weak.

Figure 5. Illustration of the Nextrom dual fiber draw tower OFC 20. (Rosendahl Nextrom Oy 2018)

At the top of the tower the preform is handled by a Nextrom Preform Feeding unit (NPF), that enables a consistent and finely controlled feeding speed into the furnace. Preform is mounted on an XY-table by a specific collar or a pin, depending on the preform. This assembly in turn is mounted on large linear guide rails for precision of movement along the Y-axis. Movement is governed by electric motors and their torque is transferred to a large diameter ball screw that dictates the movement in Z-axis. In each axis the precision of movement is in theory accurate down to 0.01 mm, which is tracked by encoders. From a practical point of view, it is easy to understand that the existence of mechanical slack creates more variance than 0.01 mm as the directions change, but this is of negligible quantity and has not been found to affect process adversely. With 150 mm preform diameter, as used

during the draws for this research, the preform feed rate at full speed of 2500 m/min is roughly 1.8 mm/min. This will vary a little bit depending on the true outside diameter of the preform. The output of optical fiber with 125 µm diameter needs to match the volume of glass being fed into the furnace to achieve equilibrium in production. Preforms commonly have many millimeters of variance in their outside diameter which leads to small differences in feeding rate.

The furnaces can be heated with few different methods, but the one used for the tests in this thesis was a bottom flow, induction heated, furnace. Here the bottom flow designates the direction of gas flow, mainly argon, that is used to prevent the graphite pieces inside the furnace from burning. Inside the furnace body is a hollow, water cooled, copper coil that carries the large current to achieve temperatures needed for melting silica-glass. The electromagnetism is induced into the graphite parts that form the walls around the preform and thus heat the glass by thermal radiation. During the process argon is continuously fed into the furnace from six different locations. These locations are:

- Top chamber, which keeps a pool of argon over the iris.
- Dynamic iris, which is a series of glass leaves that are pressurized to follow the subtle diameter variations on the surface of the preform.
- Bore, which is a graphite cylinder and the space inside which the glass melts.
- Body, which has empty space around the coil and the furnace outer shell to avoid the electromagnetism from inducing to undesired places.
- Insulator, which is a graphite felt that prevents the induced heat from the bore from melting the coil.
- Extension tube, which seals against the bottom of the furnace and regulates the cooling rate of the optical fiber.

The preform melts most efficiently at the height that is central to the coil. Induced heat is radiated from the graphite bore. Some of the heat travels outside of the furnace by means of radiated light and infrared, as well as being not entirely heat insulated. For example, the NDI is formed of two layers of glass irises that are 5 mm thick but are not insulated. Both sides of the iris leaves are saturated by argon gas to prevent oxygen from leaking to inside the furnace. As a bottom flow furnace a lot of the heat is directed downwards and out of the

extension tube. This heated argon gas travels along the same path with the fiber and regulates its rate of cooling.

The furnace temperature during the process is measured from the outside of the bores graphite wall. The device measuring the temperature is an infrared radiation based pyrometer. As the preform is located inside the graphite bore cylinder, this explains why the pyrometer measures a temperature that exceeds the melting temperature of silica-based glass. Temperature reading is difficult to achieve directly from the surface of the preform without adding considerable costs in lost energy.

At the bottom of the furnace at OFC 20 draw tower exists an extension tube. These are commonly about two meters long tubes that are made from pure quartz glass to withstand the high working temperatures. Extension tubes convey the hot argon gas that comes from the furnace and effectively regulate the heat adjacent to the fiber. Therefore, it slows down the rapid cooling of the optical fiber by keeping cool room air away from the fiber. Slowing down the cooling of the fiber is essential in reducing the amount of stress that forms inside the glass fiber as it cools down rapidly. Extension tubes are practical and cost-effective way of controlling the cooling of the fiber. Some fiber producers have taken the idea further and have been using longer two-part extension tube assemblies and insulation to presumably increase its effectiveness, especially in higher production speeds. The goal is to keep the cooling rate low enough so the forming tensions between the glass core and cladding would not change the refractive indexes and increase the intrinsic scattering of the fiber.

Next down the line comes a fiber cooling system (Figure 6). These are long water-cooled aluminum blocks that close at a predetermined line speed setpoint. While closed, the system starts to cool down the aluminum walls by circulating cool water between the cooling tubes and a chiller. Helium is fed inside these aluminum tubes, as it has a very good thermal conductivity for a gas. This fiber cooling system must cool the fiber down enough to avoid complications. High fiber temperature at the coater means that the acrylate is not grabbing onto the glass fiber as efficiently. The result can be a sticky mess as acrylate overflows the reservoir and the process must be stopped. The temperature needed to be reached after the

cooling tube is depends on the coating die and acrylate. Some die and acrylate combinations can be ok for use in 150 ^{o}C while others struggle already at 80 Celsius.

Figure 6. View upwards along the cooling tube of Nextrom Fiber Cooling System (FCS).

At this point the tensions inside the fiber is already set and further steps will have no effect on the intrinsic scattering (Rayleigh scattering) that we hope to experiment with. The winding on the spool can still affect the attenuation if the winding tension has been too high or spool is of poor quality which could cause microbending loss. Coating will get to the fiber through a die and the secondary coating will be cured inside the UV-lamps below it. As mentioned earlier, the UV-lamps provide intense ultraviolet light that causes the secondary coating to cure, or in other words harden. The UV-lamps are controlled by a power ramp setting to achieve sufficient coating during the draw in all drawing speeds. Intensity is regulated to match the time the fiber spends inside the UV-lamps. Overexposure leads to burnt acrylate coating.

Fiber is then passed by a bottom pulley and onto the main capstan. Bottom pulley is a carefully positioned wheel that needs to be in good vertical alignment with the preform. Distance from preform to this pulley in Nextrom draw tower in Vantaa is about 27 meters. The main capstan is a drive motor powered wheel with a 1.0-meter circumference. Tensioned

belt holds the fiber against the main wheel as it spins. Main capstan applies the pulling force to the fiber and gives feedback on tension and draw speed to the control unit. Last machine in order is the take-up that spools the fiber onto 1000 km reels.

3 MEASUREMENT METHODOLOGY

Draw processes aim to experiment with different extension tube lengths extension tube. In addition, each preform is considered a variable in the draw trials as their origins differ greatly. As the draw process from preform to a reel of coated fiber is a singular event, many variables can cause fluctuation in measurements. The correlation between measured data variation and the thermal profile must therefore be handled with great skepticism.

Measurements were taken from pre-determined measuring points. Each point has an XY-table mounted onto the draw tower that allows the alignment of the Sikora gauge while drawing. Correct alignment of the Sikora gauge is crucial to get reliable results as can be seen in Figure 7. The temperatures were measured with a single Sikora temperature gauge and the position was changed by hand during a live draw. The XY-tables were fitted with mechanical stops to quickly locate the Sikora gauge into a roughly correct position, which was aligned offline with a fishing line. All measurements were taken according to the following restrictions:

- The draw speed must be stable for 5 minutes prior to taken sample
- The bare fiber diameter should be within the specified 125.0 ± 0.5 µm
- The sample taken must be 2 minutes long to be considered viable
- The sample must have less than 10 % deviation to be considered viable
- Fiber tension must be stable within 10 grams variation
- Essential quality markers must be within specification in post-draw analysis with Photon Kinetics instruments

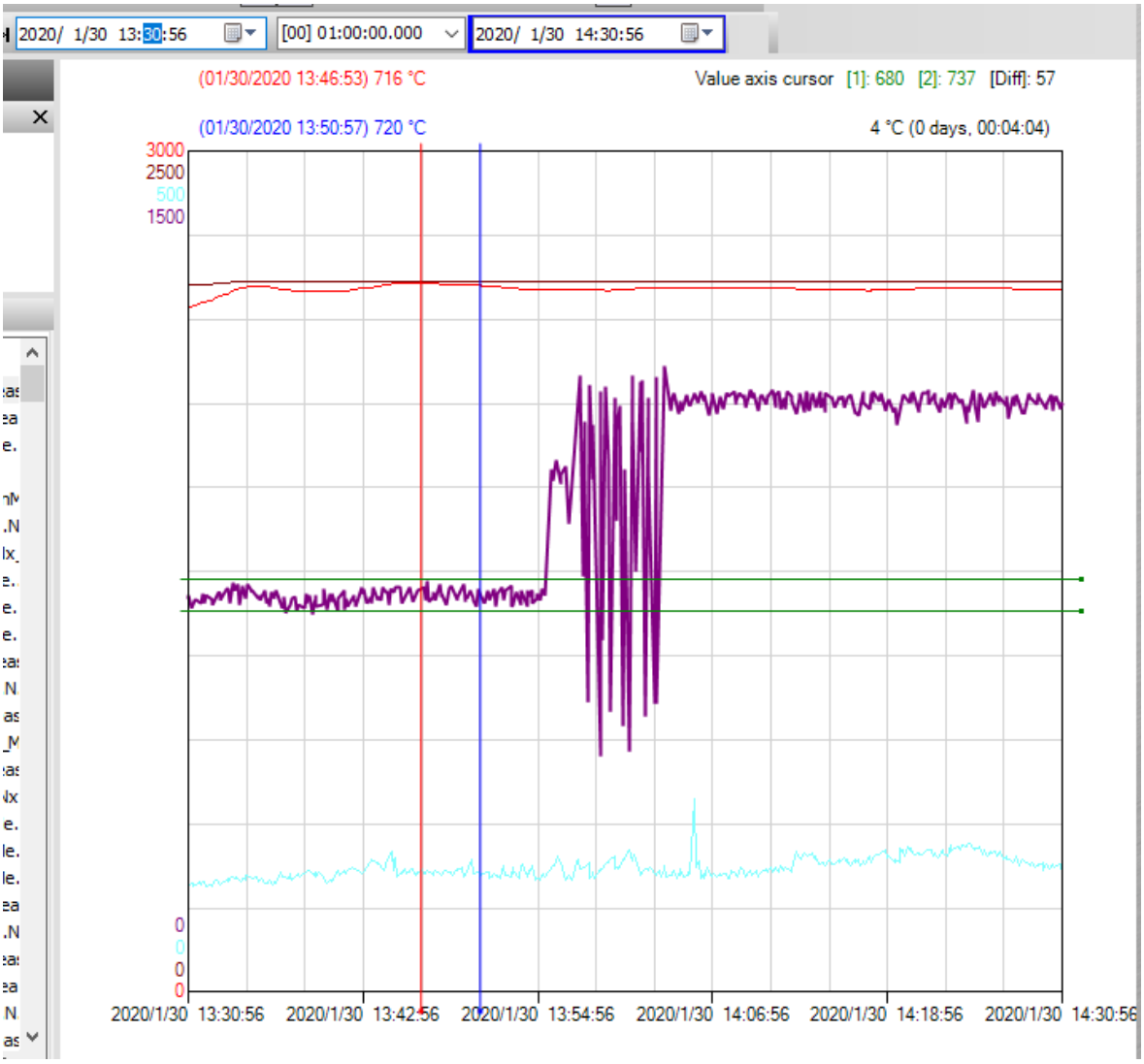

Figure 7. A close-up of transfer between measurement points. Large variance in the middle was caused by 1-2 mm of misalignment. Diameter deviation became stable after gauge position was corrected.

The locations of the surrounding devices and gauges set limitations for the plausible hot SIKORA measurement points. With varying lengths of extension tube the highest measuring point was set at 4.91 m distance from the hot zone. This distance was based on leaving enough clearance for extension tubes up to the length of three (3) meters. As a result, the variable of changing top measurement position along with the extension tube was avoided. Therefore, with every varying configuration the distance from each measuring point to the hot zone of the furnace is the same.

3.1 Sikora Hot temp gauge

The vital hot fiber temperature measurements that are the base of the whole analysis is taken with a SIKORA brand, FIBER TEMP 6003 standalone gauge (Figure 8). The gauge provides temperature reading from its thermal imaging camera. The operating principle used by SIKORA is currently patent pending (Helk 2020). When installed at the Hot positions before fiber cooling system (FCS) the measuring range of the device is 500 to 1500 ^{o}C. When the device is used after the FCS to measure the fibers cooled temperature the range is set to the range of 30 to 270 ^{o}C. The gauge is rated to the accuracy of ± 1 ^{o}C. SIKORA has designed these gauges specifically for optical fiber production. Their purpose in normal process is to provide a data point that can be referred to for optimal fiber quality. As an example, the temperature after the fiber cooling is essential to quantify the effectiveness of attempted fiber cooling and also what temperature fiber is in contact with the acrylate coating. (SIKORA webpage, 2020)

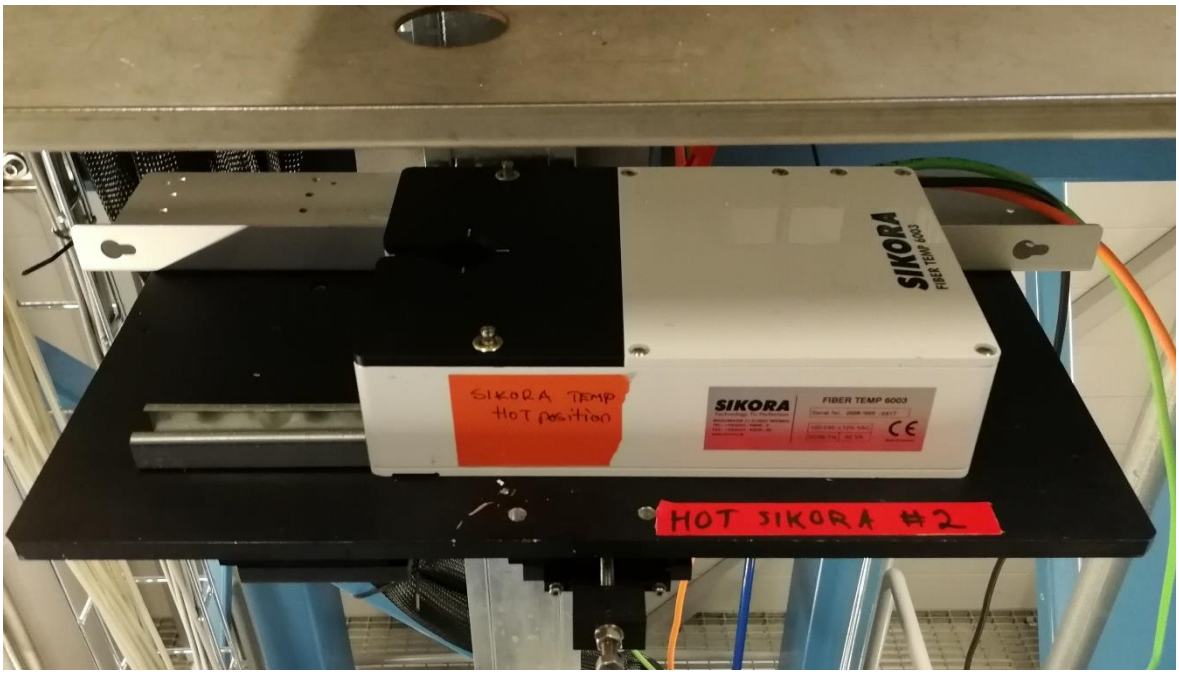

Figure 8. Hot fiber temperature measurement gauge: SIKORA FIBER TEMP 6003

As part of the line control system, at the Nextrom draw tower in Vantaa, all the SIKORA device measurements get their data stored into a central FIBER ECOCONTROL. Measurements can be viewed live as well as retrieved afterwards as the system has an

automated save function. This data is original within the SIKORA systems and is used as the source for most of the data analysis in this paper. Certain parameters like furnace power and draw speed are not visible from data saved to ECOCONTROL, which is why the Nextroms own line control and data logging program by SIKORA is used for it.

Data is processed largely inside Microsoft Excel. Sample ranges have been picked to be at least two minutes long and stable. From these intervals the local minimum, maximum and average values are calculated. Min and max values are tracked to make sure no abnormally high spikes influence the measured average, which could be missed in the graphs.

Hot SIKORA gauge has been given three different XY-table locations to measure the gradient of each draw. The position S_{H1} being the closest to the furnace and S_{H3} the furthest away from the furnace (Table 1).

Table 1. *Measured distances between the pyrometer and the gauge positions. Measurements marked in green were used to calculate the cooling rate*

Pyrometer to gauge distance	
Interval	Distance (*mm*)
Pyro -> S_{H1}	4910
Pyro -> S_{H2}	5450
Pyro -> S_{H3}	7405
Pyro -> FCS	7595
Pyro -> S_C	17295
$S_{H1} - S_{H3}$	2495
$S_{H3} \rightarrow S_C$	9890

Fiber temperature could then be used with the measured gauge distances to create a simple reference value for the rate of cooling, which would be in degrees of Celsius per second (*°C/s*). Values that needed to be tracked were $\Delta T1$, $\Delta T2$ and $\Delta T3$. Calculation was according to the following Formulas 1, 2 and 3. In the equations the T_n signifies the temperature at the same corresponding Hot Sikora position. The unit T_C stands for cold fiber diameter after the cooling tube.

$$\Delta T1 = \frac{1723\ °C - T_1}{\frac{4.91\ m}{v}} \quad (1)$$

$$\Delta T2 = \frac{T_1 - T_3}{\frac{2.495\ m}{v}} \quad (2)$$

$$\Delta T3 = \frac{T_3 - T_C}{2.495\ m} \quad (3)$$

3.2 Photon Kinetics Fiber Analysis Systems

Quality measurement of the produced optical fiber is performed on modern Photon Kinetics equipment. In 2019 the much older generation fiber analysis devices were replaced with a new complete set, which includes the 2300 series system as well as the 8000 and 2880 series as pair. This set of instruments include six different devices for wide variety of measurements. Measured parameters include:

- Spectral attenuation over the range of 1000 nm to 1650 nm (single mode fiber)
- Cutoff wavelength
- Mode Field Diameter (MFD)
- Polarization Mode Dispersion (PMD)
- Chromatic dispersion (CD)
- Complete fiber geometry measurements
    - Optical core diameter and non-circularity
    - Silica-glass cladding outer diameter and non-circularity
    - Primary coating outer diameter and non-circularity
    - Secondary coating outer diameter and non-circularity

Using the Photon Kinetics fiber analysis systems takes place in reverse order relative to the drawing process. During the draw process the last drawn optical fiber is at the top of the reel

and needs to be rewound or proof tested into smaller spools for analysis. During this rewinding the unwanted parts, like the ramp up of irregular tension between different samples can be skipped from analysis. Rewinding or proof testing is performed on another Rosendahl Nextrom device, which tracks the distance of fiber wound on to the smaller 50 or 25 km spools.

Five sets of measurements are always taken from each spool to exclude outlier values. Between each step a length of 10 meters is scrapped as part of the procedure. Purpose of the scrapping is to take samples from a larger length of fiber, thus improving the dependability of the result. These steps guarantee that the samples taken contain the bare minimum of unwanted variables that we can achieve in the existing conditions. Due to the complex process of fiber draw it is obvious that any measured results have to be carefully cross-examined for unintended affecting factors.

Measurements taken with the Photon Kinetics instruments are logged and charted together with the calculated ΔT values. After all the experiments are done the data can be analyzed to try and find any possible correlations between cooling rate and final measured attenuation and other values. With a large enough collected data set a plotted trend line can be formed and regressional analysis can be used to determine the degree of dependability for the result.

4 RESULTS

Testing results are divided into three (3) sets according to the used length of extension tube. Each set can be found later under separate subtitles in this chapter. The amount of data collected for each extension tube length was not equal in amount. In the end the longer 3.0 m and shorter 0.88 m extension tubes were performed with fewer number of test draws due to time running out.

Preforms used in each draw will be marked with an alphabet for each manufacturer and a number that designates the order number of the preform from that manufacturer. For example, “B3” means simply that the preform was the third (3^{rd}) used in the tests made by manufacturer B. Manufacturers will not be public information due to customer/collaborator confidentiality agreements.

Draws will be marked and coded according to the following system: “DYYMMDD-R”. Here the YY is the last two digits of the year, MM are months and DD are days. The last designation “-R” refers to the reel order number. It does not mean that a full 1000km reel of optical fiber was drawn on that day, but that the reel was simply changed. This is a practical feature to access the desired optical fiber quicker for post-draw measurements on the Photon Kinetics machines. Further alphabetical number, as in D200416-1-A means the rewound small reel that is usually 25 or 50 kilometers of fiber.

Measurement points themselves are numbered top to bottom. Temperature *T1* is the hottest and closest to the extension tube at the top. The *T2* is in the middle and the *T3* is lowest and closest to cooling tube. Cooling rate values are simple calculated values. Calculation formula (1) can be found in chapter 3.1. Cooling rate $\Delta T2$ is the temperature gradient between the highest and lowest Hot gauge measurements points. Cooling rate $\Delta T3$ is the gradient between the lowest Hot gauge measurement and the Cold gauge. Cooling rates are adjusted to the

drawing speed in each process. The final result is aimed to portray a clear time-related rate of cooling with unit being “Celsius degrees per second”.

4.1 Medium length extension tube

The first sample set was taken with the standard 2.05 m extension tube length. There were 6 different draws from which the thermal profile was taken with seven (7) separate data sets. During the draw of D200416 there were two (2) separate data sets with different tensions made. More draws had been made, but several draws during February and March were with mechanical quality preforms, which had no doped core glass. These draws had to be omitted. Further draws had two preforms that resulted in highly irregular core glass measurements, once quality was examined with the PK machines, that also needed to be excluded from the draws. These excluded draws resulted in a delay in the schedule of the made draws for this research, as well as lost resources.

Process during D200128 was drawn with preform from manufacturer “A”, which has a good reputation for quality. Below (Tables 2 & 3) you can see the measured averages from this draw.

Table 2. *Draw D200128 measured average values.*

Draw code	**Attenuation** ***1310 nm (dB/km)***	**Attenuation** ***1550 nm (dB/km)***	***T1 (°C)***	***T2 (°C)***	***T3 (°C)***	***Tc (°C)***	***ΔT1 (°C/s)***	***ΔT2 (°C/s)***
D200128-2	0.329	0.185	1005	847	689	74	6093	5277

Table 3. *Logged D200128 draw parameters.*

Extension tube length ***(m)***	**Draw speed** ***(m/min)***	**Tension** ***(N)***	**Furnace power (k*W*)**	**Preform**	**Preform OD** ***(mm)***	**Acrylates**	**Die**
2.05	2500	1.09	40.4	A	150	DP-1077 & DS-2088	ZL3

The drawing of D200130 happened with preform from a reputable manufacturer "A". Below (Tables 4 & 5) you can see the measured averages from this draw.

Table 4. *Draw D200130 measured average values.*

Draw code	Attenuation *1310 nm (dB/km)*	Attenuation *1550 nm (dB/km)*	*T1 (°C)*	*T2 (°C)*	*T3 (°C)*	*Tc (°C)*	*ΔT1 (°C/s)*	*ΔT2 (°C/s)*
D200130-2	0.329	0.187	1055	921	701	75	5691	5935

Table 5. *D200130 draw measured parameters.*

Extension tube length *(m)*	Draw speed *(m/min)*	Tension *(N)*	Furnace power (k*W*)	Preform	Preform OD *(mm)*	Acrylates	Die
2.05	2510	1.01	39.9	A	150	DP-1077 & DS-2088	W015

Draw D200331 was done with the 1st preform from manufacturer B. Below in Tables 6 & 7 you can see the measured average value and parameters for this draw. During the draw the bare fiber diameter was spiking out of the specified 125 ± 0.5 µm variation. The coating also had concentricity issues when measured with Photon Kinetics instruments, but small centricity issue in coating is unlikely to cause any changes to attenuation.

Table 6. *Draw D200331 measured average values.*

Draw code	Attenuation *1310 nm (dB/km)*	Attenuation *1550 nm (dB/km)*	*T1 (°C)*	*T2 (°C)*	*T3 (°C)*	*Tc (°C)*	*ΔT1 (°C/s)*	*ΔT2 (°C/s)*
D200331-4	0.329	0.185	1054	942	734	73	5677	5344

Table 7. *D200131 draw measured parameters.*

Extension tube length *(m)*	Draw speed *(m/min)*	Tension *(N)*	Furnace power (k*W*)	Preform	Preform OD *(mm)*	Acrylates	Die
2.05	2500	0.61	36.2	B1	147	DP-1077 & DS-2088	Z011

The D200401 process was drawn with the 1st preform from a manufacturer "B" as on 31st of March. Said preform was a short because of earlier trials. This meant that only a small portion of the preform was above the insertion depth was usable prior to touchdown event. Touchdown happened in the middle of the draw. Below (Tables 8 & 9) you can see the measured averages from this draw.

Table 8. *Draw D200401 measured average values.*

Draw code	Attenuation *1310 nm (dB/km)*	Attenuation *1550 nm (dB/km)*	*T1 (°C)*	*T2 (°C)*	*T3 (°C)*	*Tc (°C)*	*ΔT1 (°C/s)*	*ΔT2 (°C/s)*
D200401	0.327	0.183	1063	944	721	72	5601	5711

In the middle of the draw the touchdown sequence was reached. This means that the top of the preform is sealed by a quartz cylinder as the preform is too short to seal the top opening. As a result, the glass volume inside the furnace gets smaller and less heat is lost as outward thermal radiation. This all equates to smaller than normal kilowatt count inside the furnace.

Table 9. *D200401 draw measured parameters.*

Extension tube length *(m)*	Draw speed *(m/min)*	Tension *(N)*	Furnace power (k*W*)	Preform	Preform OD *(mm)*	Acrylates	Die
2.05	2500	1.17	32.1	B1	147	DP-1077 & DS-2088	Z011

D200402 was drawn with the final portion of the 1st preform from a manufacturer "B". The draw started within 1st touchdown depth. Below (Tables 10 & 11) you can see the measured averages from this draw.

Table 10. *Draw D200402 measured average values.*

Draw code	Attenuation *1310 nm (dB/km)*	Attenuation *1550 nm (dB/km)*	*T1 (°C)*	*T2 (°C)*	*T3 (°C)*	*Tc (°C)*	*ΔT1 (°C/s)*	*ΔT2 (°C/s)*
D200402	0.328	0.184	1023	910	704	69	5940	5327

During this draw the preform B1 was finished. This meant that the 2nd touchdown happened during the draw. This resulted in a much lower average kilowatt count inside furnace to achieve the same tension at the same 2500 m/min.

Table 11. *D200402 draw measured parameters. Notice the much lower furnace power as a result of the end draw.*

Extension tube length *(m)*	Draw speed *(m/min)*	Tension *(N)*	Furnace power (k*W*)	Preform	Preform OD *(mm)*	Acrylates	Die
2.05	2500	1.05	30.7	B1	147	DP-1077 & DS-2088	Z011

During draw D200416 the process was drawn with the 2nd preform from a manufacturer "B". Below (Tables 12, 13, 14 & 15) you can see the measured averages from this draw. The different ending "-1-A" and "-1-C" of the draw codes refers to the separate samples of the draw, which was done at different target tensions.

Table 12. *Draw D200416-1-A measured average values.*

Draw code	Attenuation *1310 nm (dB/km)*	Attenuation *1550 nm (dB/km)*	*T1 (°C)*	*T2 (°C)*	*T3 (°C)*	*Tc (°C)*	*ΔT1 (°C/s)*	*ΔT2 (°C/s)*
D200416-1-A	0.331	0.183	951	845	625	59	5372	4464

Table 13. *D200416-1-A draw measured parameters.*

Extension tube length *(m)*	Draw speed *(m/min)*	Tension *(N)*	Furnace power (k*W*)	Preform	Preform OD *(mm)*	Acrylates	Die
2.05	2050	0.71	38.4	B2	148	DP-1077 & DS-2088	Z011

The second measurements of the same draw with a larger tension target. This is why the furnace power is different between -A and -C samples reels. Less power and heat results in more tension.

Table 14. *Draw D200416-1-C measured average values.*

Draw code	Attenuation *1310 nm (dB/km)*	Attenuation *1550 nm (dB/km)*	*T1 (°C)*	*T2 (°C)*	*T3 (°C)*	*Tc (°C)*	*ΔT1 (°C/s)*	*ΔT2 (°C/s)*
D200416-1-C	0.331	0.174	942	837	609	55	5434	4560

Table 15. *D200416-1-C draw measured parameters.*

Extension tube length *(m)*	Draw speed *(m/min)*	Tension *(N)*	Furnace power (k*W*)	Preform	Preform OD *(mm)*	Acrylates	Die
2.05	2050	1.00	35.9	B2	148	DP-1077 & DS-2088	Z011

4.2 Long extension tube

The Second sample set was performed with a longer 3.0 m extension tube. Compared to the standard length 2.05 m long extension tube, the temperature that fiber has as it exits the extension tube is almost immediately measured by the top SIKORA gauge. There is still about 0.40 meters of free fiber length at room temperature, but this is only 29.6 % of the previous free fiber length with the standard medium length tube. The 0.95 meter of missing

free length can clearly be seen in measured temperatures. Long extension tube was tested only with a total of three valid draw measurement sets.

Draw D200421 was the first time the process with the long extension tube was started with the same B2 preform as D200416 draw. Target tension for the draw was standard 1.0 Newton. The target speed was between 2000 and 2100 m/min and other changes were not made. Results and measured values can be seen below (tables 16 & 17).

Table 16. *Draw D200421 measured average values.*

Draw code	Attenuation *1310 nm (dB/km)*	Attenuation *1550 nm (dB/km)*	*T1 (°C)*	*T2 (°C)*	*T3 (°C)*	*Tc (°C)*	*ΔT1 (°C/s)*	*ΔT2 (°C/s)*
D200421	0.329	0.171	1086	973	714	65	4486	5156

Table 17. *D200421 draw measured parameters.*

Extension tube length *(m)*	Draw speed *(m/min)*	Tension *(N)*	Furnace power (k*W*)	Preform	Preform OD *(mm)*	Acrylates	Die
3.0	2075	0.97	36.3	B2	148	DP-1077 & DS-2088	Z011

Draw D200430 was done on April 30th. It was started with the 3rd preform from the manufacturer “B”. Below are Tables 18 & 19 with the measured values. Draw was done at 2500 m/min and target tension of 1,0 newtons which was achieved exactly. Die had been changed from Z011 to ZL3 in an attempt to have more acrylate flow with less line pressure. This can only effect final dimensions of coating and should not have any effect on attenuation. Furnace power varied a bit over 2 kW during the draw, which is a direct consequence of a touchdown sequence and preform starting to end.

Table 18. *Draw D200430 measured average values.*

Draw code	Attenuation *1310 nm (dB/km)*	Attenuation *1550 nm (dB/km)*	*T1 (°C)*	*T2 (°C)*	*T3 (°C)*	*Tc (°C)*	*ΔT1 (°C/s)*	*ΔT2 (°C/s)*
D200430	0.329	0.184	1216	1045	825	77	4302	6529

Table 19. *D200430 draw measured parameters.*

Extension tube length *(m)*	Draw speed *(m/min)*	Tension *(N)*	Furnace power (k*W*)	Preform	Preform OD *(mm)*	Acrylates	Die
3.0	2500	1.00	37.5 – 35.1	B3	150	DP-1077 & DS-2088	ZL3

In the draw D200507 the acrylate materials were changed due to a customer related project. Target of the draw was 90-100 grams of tension at around 2000 m/min draw speed. Change of acrylates should not have affected measured attenuation values and such changes are counted as negligible. Measured average values (Tables 20 & 21) are below.

Table 20. *Draw D200507 measured average values.*

Draw code	Attenuation *1310 nm (dB/km)*	Attenuation *1550 nm (dB/km)*	*T1 (°C)*	*T2 (°C)*	*T3 (°C)*	*Tc (°C)*	*ΔT1 (°C/s)*	*ΔT2 (°C/s)*
D200507	0.326	0.183	1055	937	716	71	4580	4574

Table 21. *D200507 draw measured parameters.*

Extension tube length *(m)*	Draw speed *(m/min)*	Tension *(N)*	Furnace power (k*W*)	Preform	Preform OD *(mm)*	Acrylates	Die
3.0	2020	0.88	30.5	B3	150	DP-1032 & DS-2042	ZL3

4.3 Short extension tube

The third and final experiment set was done with a much shorter 0.88 m extension tube. Goal of this set was to force any possible differences in fiber quality measurements. There was 86.7 % longer free fiber length when compared to the medium length extension tube, as the free length extended from 1.35 to 2.52 meters. Temperature measurements from the fiber are considerably lower due to longer exposure to room temperature. Due to time restrictions, in the form of thesis deadlines, only 2 draws were made with the 0.88 m extension tube. However, both draws were very successful and from them multiple measurements were made in multiple draw speeds. This enabled even some draw speed related comparison that was before not collected.

The draw D200528-2-B was with the 4th preform by manufacturer B. This is chronologically the first draw with the very short 0.88 m extension tube. This draw finished the preform B4 and had touchdown event during the draw that changed the kilowatts needed in furnace during the draw. Measurements are found below in Tables 22 and 23.

Table 22*. Draw D200528-2-B measured average values.*

Draw code	Attenuation *1310 nm (dB/km)*	Attenuation *1550 nm (dB/km)*	*T1 (°C)*	*T2 (°C)*	*T3 (°C)*	*Tc (°C)*	*ΔT1 (°C/s)*	*ΔT2 (°C/s)*
D200528-2-B	0.328	0.184	854	778	615	67	7395	4002

Table 23. *D200528-2-B draw measured parameters.*

Extension tube length *(m)*	Draw speed *(m/min)*	Tension *(N)*	Furnace power (k*W*)	Preform	Preform OD *(mm)*	Acrylates	Die
0.88	2507	0.71	31.3	B4	150	DP-1032 & DS-2042	ZL3

The draw D200528-2-D was measured from same draw as D200528-2-B, but with slower draw speed. No fiber cut had occurred in between measurements, as speed was simply ramped down to around 2000 m/min. This is chronologically part of the same the first draw

with the very short 0.88 meter extension tube. Measured data from draw is in Tables 24 and 25 below.

Table 24. *Draw D200528-2-D measured average values.*

Draw code	**Attenuation** ***1310 nm (dB/km)***	**Attenuation** ***1550 nm (dB/km)***	***T1 (°C)***	***T2 (°C)***	***T3 (°C)***	***Tc (°C)***	***ΔT1 (°C/s)***	***ΔT2 (°C/s)***
D200528-2-D	0.327	0.183	758	674	507	48	6570	3363

Table 25. *D200528-2-D draw measured parameters.*

Extension tube length ***(m)***	**Draw speed** ***(m/min)***	**Tension** ***(N)***	**Furnace power (k*W*)**	**Preform**	**Preform OD** ***(mm)***	**Acrylates**	**Die**
0.88	2006	0.66	32.8	B4	150	DP-1032 & DS-2042	ZL3

The draw D200604-1-E was with the 5th preform by manufacturer B. This is chronologically the first fiber sample on the 1000 km reel during draw D200604. This draw (D200604) started and finished the preform B5 with no fiber breaks. Touchdown event happened during the draw that changed the kilowatts needed in furnace during the draw. Measurements are found below in Tables 26 and 27.

Table 26. *Draw D200604-1-E measured average values.*

Draw code	**Attenuation** ***1310 nm (dB/km)***	**Attenuation** ***1550 nm (dB/km)***	***T1 (°C)***	***T2 (°C)***	***T3 (°C)***	***Tc (°C)***	***ΔT1 (°C/s)***	***ΔT2 (°C/s)***
D200604-1-E	0.342	0.190	767	676	513	51	6545	3422

Table 27. *D200604-1-E draw measured parameters.*

Extension tube length *(m)*	Draw speed *(m/min)*	Tension *(N)*	Furnace power (k*W*)	Preform	Preform OD *(mm)*	Acrylates	Die
0.88	2017	0.74	33.1	B5	150	DP-1032 & DS-2042	ZL3

The draw D200604-1-C was with the same preform as all draws in D200604. This is chronologically the 2nd fiber sample to be spooled onto the 1000 km reel during draw process. Below are measured values in Tables 28 and 29. Measured temperature values T1, T2, T3 and Tc are same as on spool D200604-1-E because both of the samples were recorded from same stable production phase at roughly 2000 m/min. Sample are still separate 40 km long spools that were analyzed by PK machine individually. Differences in *ΔT1* and *ΔT2* values from each spool of the same draw come from small line speed variation, which is one of the variables used to calculate these variables.

Table 28. *Draw D200604-1-C measured average values.*

Draw code	Attenuation *1310 nm (dB/km)*	Attenuation *1550 nm (dB/km)*	*T1 (°C)*	*T2 (°C)*	*T3 (°C)*	*Tc (°C)*	*ΔT1 (°C/s)*	*ΔT2 (°C/s)*
D200604-1-C	0.344	0.191	767	676	513	51	6535	3417

Table 29. *D200604-1-C draw measured parameters.*

Extension tube length *(m)*	Draw speed *(m/min)*	Tension *(N)*	Furnace power (k*W*)	Preform	Preform OD *(mm)*	Acrylates	Die
0.88	2014	0.71	33.1	B5	150	DP-1032 & DS-2042	ZL3

The draw D200604-1-A was in order the 4th fiber sample on the main reel during the process. Below are measured values in Tables 30 and 31. Spool -1-A was drawn with higher draw speed of 2530 (average over the sample period).

Table 30. *Draw D200604-1-A measured average values.*

Draw code	Attenuation *1310 nm (dB/km)*	Attenuation *1550 nm (dB/km)*	*T1 (°C)*	*T2 (°C)*	*T3 (°C)*	*Tc (°C)*	*ΔT1 (°C/s)*	*ΔT2 (°C/s)*
D200604-1-A	0.345	0.193	872	783	617	66	7308	4310

Table 31. *D200604-1-A draw measured parameters.*

Extension tube length *(m)*	Draw speed *(m/min)*	Tension *(N)*	Furnace power (k*W*)	Preform	Preform OD *(mm)*	Acrylates	Die
0.88	2530	0.65	31.4	B5	150	DP-1032 & DS-2042	ZL3

The draw D200604-2-A was in order the 5th and last fiber sample on the main reel during the process of the D200604 draw. Below are measured values in Tables 32 and 33. Spool -2-A was drawn with much lower draw speed of 1517 m/min that is a calculated average over the sample period.

Table 32. *Draw D200604-2-A measured average values. (* The T3 value was an estimation as the minimum range Sikora is able to receive is 400 Celsius and no actual measurement could be taken. The number 370 was deduced from seeing around 400 Celsius peak readings and subtracting the average ± 30 °C deviation from that.)*

Draw code	Attenuation *1310 nm (dB/km)*	Attenuation *1550 nm (dB/km)*	*T1 (°C)*	*T2 (°C)*	*T3 (°C)*	*Tc (°C)*	*ΔT1 (°C/s)*	*ΔT2 (°C/s)*
D200604-2-A	0.348	0.194	618	534	370*	48	5690	2513

Abnormally the draw speed was set to a target of 1500 m/min after results of D200528. However, the poor results were simply due to an issue in reliability with the PK measurement devices. Reliability issue was managed to a degree, after D200604. As a result, an extra speed setpoint was measured at the end of the draw. This provides data of interest when comparing attenuation values of same preform from three different speed setpoints.

Table 33. *D200604-2-A draw measured parameters.*

Extension tube length *(m)*	**Draw speed *(m/min)***	**Tension *(N)***	**Furnace power (k*W*)**	**Preform**	**Preform OD *(mm)***	**Acrylates**	**Die**
0.88	1517	0.86	27.5	B5	150	DP-1032 & DS-2042	ZL3

5 ANALYSIS OF RESULTS

As explained earlier the measurements of all three hot Sikora positions and cold Sikora position were taken on each fiber draw for tracking of the fibers cooling rate. Additionally, multiple parameters were needed to take under observation in order to easily see main external factors. For example, furnace power can be lower for several reasons and this can be seen in *T* temperature values. Notes were of course made for events like end draw, which includes further sealing of the furnace top that will lower the demand of power as will the resulting lower glass mass inside the furnace. End draw process also will restrict some of the thermal radiation from radiating outward from the top of the furnace.

A major and unfortunate issue with the collected data in this research is the amount of used preforms and their quality. These tests were done with what was available to us during the spring of 2020. That meant using only old leftover preforms that were extremely short. Shortness of the preform caused an additional variable between most of the draws, in turn obviously makes it more difficult to find a cause for differences in quality with any great degree of certainty.

5.1 Cooling rate

When comparing certain end draw samples with regular draws, the difference is not noticeable from the cooling rate values. In the 2.05 m length samples the cooling rates have differences in the D200416 draw results. From the Table 34 we can see that specially the cooling rate *ΔT2* and *ΔT3* have abnormally low values compared to measurements in other draws. The cooling rate is obviously a result of the lower drawing speed of ~2050 m/min compared to the 2500 m/min. This is logical as a higher drawing speed means the fiber has less time to cool from melt temperature until the gauges. Therefore, the gradient is higher once the fiber is outside the shielding heat of the extension tube. This can be most clearly seen in *ΔT3* of each draw, as the cooled helium gas inside the FCS has more time for heat exchange.

Table 34. *Comparative Table of cooling rates for 2.05 m length extension tube draws. In the Table ΔT1 is rate of cooling between furnace melt position and 1st hot gauge, ΔT2 is the cooling rate between the first and last hot gauges and finally the ΔT3 shows us the cooling rate between last hot gauge and the cold temperature gauge, which is located right under the FCS.*

Draw code	*T1 (°C)*	*T2 (°C)*	*T3 (°C)*	*Tc (°C)*	*ΔT1 (°C/s)*	*ΔT2 (°C/s)*	*ΔT3 (°C/s)*
D200128-2	1005	847	689	74	6093	5277	2591
D200130-2	1055	921	701	75	5691	5935	2648
D200331-4	1054	942	734	73	5677	5344	2785
D200401	1063	944	721	72	5601	5711	2734
D200402	1023	910	704	69	5940	5327	2675
D200416-1-A	951	845	625	59	5383	4473	1959
D200416-1-C	942	837	609	55	5440	4565	1916

The number of successful draws with the 3.0 m extension tube was left to only three. Coating issues, failed draw attempts and other non-related R&D work that happened during late April and most of May prevented collection of larger amounts of data. Luckily the 3.0 m tube is perhaps the least crucial length to be examined. As a consequence of small sample set and having quite large deviance in calculated cooling rates, this is the least dependable data in this research. In the draw D200430 the draw speed is 2500 m/min compared to the 2020 m/min and 2080 m/min of the other two. This higher draw speed means that the fiber exits the extension tube hotter and will therefore cool a lot faster once outside of the glass extension tube that has maintained its temperature.

Table 35. *Comparative Table of cooling rates for 3.0 m length extension tube draws.*

Draw code	*T1 (°C)*	*T2 (°C)*	*T3 (°C)*	*Tc (°C)*	*ΔT1 (°C/s)*	*ΔT2 (°C/s)*	*ΔT3 (°C/s)*
D200421	1086	973	714	65	4497	5169	2275
D200430	1216	1045	825	77	4302	6530	3151
D200507	1055	937	716	71	4580	4574	2196

Table 36. *Comparative Table of cooling rates for 0.88 m length extension tube draws. (*The yellow highlighted square is an estimation. Sikora minimum reading level is 400 Celsius. Value 370 came from estimation of ± 30 °C deviation and still seeing occasional 400+ degree reading in Sikora as part of the natural deviation)*

Draw code	*T1 (°C)*	*T2 (°C)*	*T3 (°C)*	*Tc (°C)*	*ΔT1 (°C/s)*	*ΔT2 (°C/s)*	*ΔT3 (°C/s)*
D200528-2-B	854	778	615	67	7395	4002	2315
D200528-2-D	758	674	507	48	6571	3363	1552
D200604-1-E	767	676	513	51	6545	3422	1570
D200604-1-C	767	676	513	51	6536	3417	1568
D200604-1-A	872	783	617	66	7308	4310	2349
D200604-2-A	618	534	370*	48	5690	2513	823

The Standard deviation in 2000 m/min draws looks very consistent for most of the measured data. The *ΔT2* between top and bottom Hot SIKORA positions looks somewhat irregular only on the 3.0-meter-long extension tube (Table 37). This difference to have no obvious reasons. Difference in draw speed between D200421 and D200507 is 60 m/min, which is 1 m/s. That is a mere 3.0 % difference from the target speed of each draw. The temperature differences between *T1* and *T3* for draws D200421 and D200507 are 372 and 339 *°C* respectively. Because there is no other draws with 2000 m/min target speed and 3.0 m extension tube, it is hard to say which is irregular. Both draws also have different preforms,

B2 and B3 which is likely to be an obvious contributor. Furthermore, the preform B2, with its unusually low attenuation at 1550 nm, is likely to have an irregular silica-core composition. This idea is somewhat supported by the fact that the measure furnace power consumption was abnormally high at 36,3 kW when we consider that the preform was under touchdown depth and ending exactly during the D200421 draw. By comparison the power needed inside the furnace during the D200507 draw was 30.5 kW, while maintaining similar target speed and tension between these two draws only had a difference of 0.09 Newtons.

Table 37. *Calculated standard deviation values at 2000 M/MIN for each set of cooling rate measurements.*

Deviation at 2000 M/MIN			
Length	STDEV *ΔT1 (°C/s)*	STDEV *ΔT2 (°C/s)*	STDEV *ΔT3 (°C/s)*
3.00	41.4	297.2	39.6
2.05	28.7	45.8	21.7
0.88	14.9	26.6	8.3

At 2000 m/min in the 2.05 m tube group the values for *ΔT2* are around the average of 4519 °C/s with 45.8 °C/s of standard deviation (Tables 34 & 37). By percentage this calculates to 1.01 % deviation. At the same time at 2500 m/min speed the average is 5519 °C/s but the deviation is a greater 259.3 °C/s. This is considerably more with its 4.69 % deviation than the earlier 1.01 %. However, the under 5 % deviation is still not completely invalid as a result. At most it gives a suspicion to how a longer preform for multiple data setpoints could prove more effective in finding out smaller differences that are obscured by excessive variables like constantly changing preform. When comparing Tables 37 and 38 a trend is visible that deviation increases along with the process speed.

Table 38. *Calculated standard deviation values at 2500 M/MIN for each set of cooling rate measurements. With 3.0 m extension tube length only one draw was made at 2500 M/MIN, which allows no deviation to be calculated.*

Deviation at 2500 M/MIN			
Length	STDEV *ΔT1 (°C/s)*	STDEV *ΔT2 (°C/s)*	STDEV *ΔT3 (°C/s)*
3.00	-	-	-
2.05	185.5	259.3	67.3
0.88	43.4	153.6	17.0

Main factors that can cause differences in calculated standard deviation values are furnace power as well as the line speed. Furnace power, and therefore final bare fiber tension, may be different simply due to inconsistent line ramp up. When accelerating the line to target speed by hand, it is easy to have some human error. Final target tension should dictate final furnace temperature already early during the ramp up. Commonly 500 M/MIN is the speed at which the final furnace temperature should already be set. Prior to development of Nextrom Autoramp (April and May 2020) the final tension was harder to predict beforehand. Any late changes to the furnace temperature would have caused a rapid change to line speed, which in turn would cause a big delay when trying to stabilize the line speed back to the targeted value.

Cooling rate *ΔT3* is also influenced by the total Helium flow activity of the FCS. In draw D200416 the draw speed is 2050 in contrast with every other draw having the speed 2500 m/min. How the helium total flow ramp is set up will affect this value. Highest helium flow setpoint in the stepped ramp is commonly 2000 m/min. This means that the draws at 2500 m/min and 2050 m/min have same exact helium flow inside the cooling tubes, despite carrying very different thermal loads. With a 2.05m extension tube 2500 m/min draws measure roughly 100 degrees Celsius more at each hot measurement point than in the 2050 m/min draw, and almost 150 degrees Celsius with the 3.0 m extension tube. With the 0.88 m extension tube the difference at the same speeds stays at 100 °C.

5.2 Attenuation comparison

When comparing the long and the medium length extension tubes, there are only two big deviations in attenuation (Table 39). Much of the draws fall within margin of 1.6 % in the 1550 nm range. Variation for the 1310 nm range is even smaller at 0.9 %. For both the deviation in attenuation of ± 0.002 dB/km is insignificant with the number of samples and uncontrolled external factors this study. Quality control in the existing R&D environment, changing preforms and other simultaneously ongoing projects all make it challenging to draw conclusions from such fine differences.

Table 39. *Long (3.0 m) and medium length (2.05 m) extension tube draw attenuations.*

Draw code	Attenuation *1310 nm (dB/km)*	Attenuation *1550 nm (dB/km)*	*ΔT1 (°C/s)*	*ΔT2 (°C/s)*	*ΔT3 (°C/s)*
D200128-2	0.329	0.185	6093	5277	2591
D200130-2	0.329	0.187	5691	5935	2648
D200331-4	0.329	0.185	5677	5344	2785
D200401	0.327	0.183	5601	5711	2734
D200402	0.328	0.184	5940	5327	2675
D200416-1-A	0.331	0.183	5383	4473	1959
D200416-1-C	0.331	0.174	5440	4565	1916
D200421	0.329	0.171	4497	5169	2275
D200430	0.329	0.184	4302	6530	3151
D200507	0.326	0.183	4580	4574	2196

Examining Table 39 in the results chapter reveals to us that the attenuation values for D200416-1-C and D200421 were exceptionally low 0.174 and 0.171 dB/km respectively. The likely cause of this value difference is the preform “B2”. Draw D200421 was executed with a 3.0 m long extension tube while D200416-1-C was with the 2.05 m tube. Because of the drastic difference in extension tube lengths, the final calculated cooling rate values were also very different. However, the spool -1-A of draw D200416 had a rather usual attenuation of 0.183 dB/km. All three samples had the draw speed between 2050 to 2080 meters per minute.

Draws D200416 and D200421 had both the same preform B2. All other measured parameters seem to not have any abnormalities when compared to other draws. Both draws had slower draw speeds at 2050 and 2075 m/min respectively. Extension tube lengths were different between the draws as were the cooling rate *ΔT1* values. This supports the idea that the single most dominant factor is the preform itself. It is possible that the preform B2 was a high-quality mechanical preform. Through collaboration with company B, Nextrom receives at times preforms as a favor or at a big discount. The quality of the preforms is usually not guaranteed, even though firsthand experience implies their quality to surpass some competition even with such disclaimers. If the core in this preform had irregular doping or no doping, the lower attenuation could be explained. Germanium doping in the core increases the silica glass cores refractive index, but also increases the loss. Lack of germanium in the core could be the cause of the preforms exceptionally low attenuation at 1550 nm.

Table 40. *Short (0.88 m) and medium length (2.05 m) extension tube draw attenuations.*

Draw code	**Attenuation** ***1310 nm (dB/km)***	**Attenuation** ***1550 nm (dB/km)***	***ΔT1 (°C/s)***	***ΔT2 (°C/s)***	***ΔT3 (°C/s)***
D200128-2	0.329	0.185	6093	5277	2591
D200130-2	0.329	0.187	5691	5935	2648
D200331-4	0.329	0.185	5677	5344	2785
D200401	0.327	0.183	5601	5711	2734
D200402	0.328	0.184	5940	5327	2675
D200416-1-A	0.331	0.183	5383	4473	1959
D200416-1-C	0.331	0.174	5440	4565	1916
D200528-2-B	0.328	0.184	7395	4002	2315
D200528-2-D	0.327	0.183	6571	3363	1552
D200604-1-E	0.342	0.190	6545	3422	1570
D200604-1-C	0.344	0.191	6536	3417	1568
D200604-1-A	0.345	0.193	7308	4310	2349
D200604-2-A	0.348	0.194	5690	2513	823

By changing the length of the extension tube, we have simply attempted to moderate the cooling rate values as presented thus far. That is why simply talking about the length of the extension tube is not sufficient to fully understand the reason of changes in attenuation. Cooling rate can be affected by many parameters like drawing speed, furnace power, length of extension tube and the insulation of extension tube. What is then fundamental to understand is the relationship between attenuation and the rate at which the fiber cools down.

The relationship between the calculated cooling rate values and the measured attenuation at 1550 nanometers is shown below in the Figure 9. As one can see the two abnormally measurements of attenuation are positioned far below rest of the group. Cooling rate data is color coded between *ΔT1*, *ΔT2* and *ΔT3*. Data here is mixed between all extension tube lengths and all draws. Dashed trend lines show us clearly that the *ΔT1* has a positive relationship with the plotted cooling rate data, while *ΔT2* and *ΔT3* are inversely related. However, it is important to keep in mind that the data presented in Figure 9 is not proving causation but simple correlation. That is why each of the cooling rate phases must be analyzed individually. It is also obvious that the data has scattered quite much.

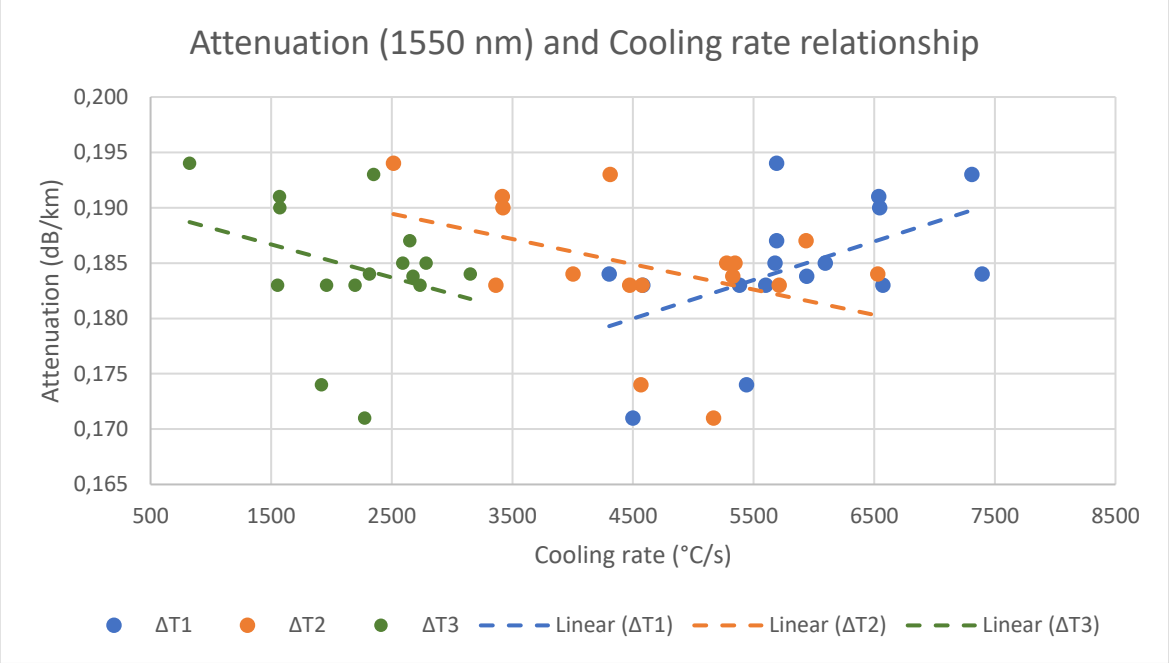

Figure 9. Plotted data from the relationship of cooling rate (X-axis) and attenuation (Y-axis) Displayed data contains all draws and all extension tube lengths.

Theoretically the intrinsic scattering, that is the result of tensions inside the optical fiber that cause changes in refractive indexes, is already set during the phase between furnace melt point and first hot SIKORA gauge to measure temperature from the fiber. The value *ΔT1* used to describe the cooling rate in that phase is then the most essential of the three cooling rate values. From Table 40 we can see that the lower attenuation values are achieved by longer extension tubes and conversely the short extension tube resulted in higher measured attenuation at 1550 nm. This idea of controlled cooling is visualized in Figure 10. Between the "Melt to gauges" and "Between hot gauges", which are *ΔT1* and *ΔT2* respectively, the cooling rate values change over. With longer 3.0 m cooling tube the free length from extension tube to 1st hot gauge position is 0.40 m and the hot optical fiber has had very short time to interact with room temperature. At the speed of 2500 M/MIN this time is 9.6 milliseconds. When drawing at same speed with 0.88 m extension tube, which results in 2.52 meters of free length before 1st SIKORA, the time of exposure is 60.4 milliseconds. That is 629 % increase in exposed time before first measurement at *T1*.

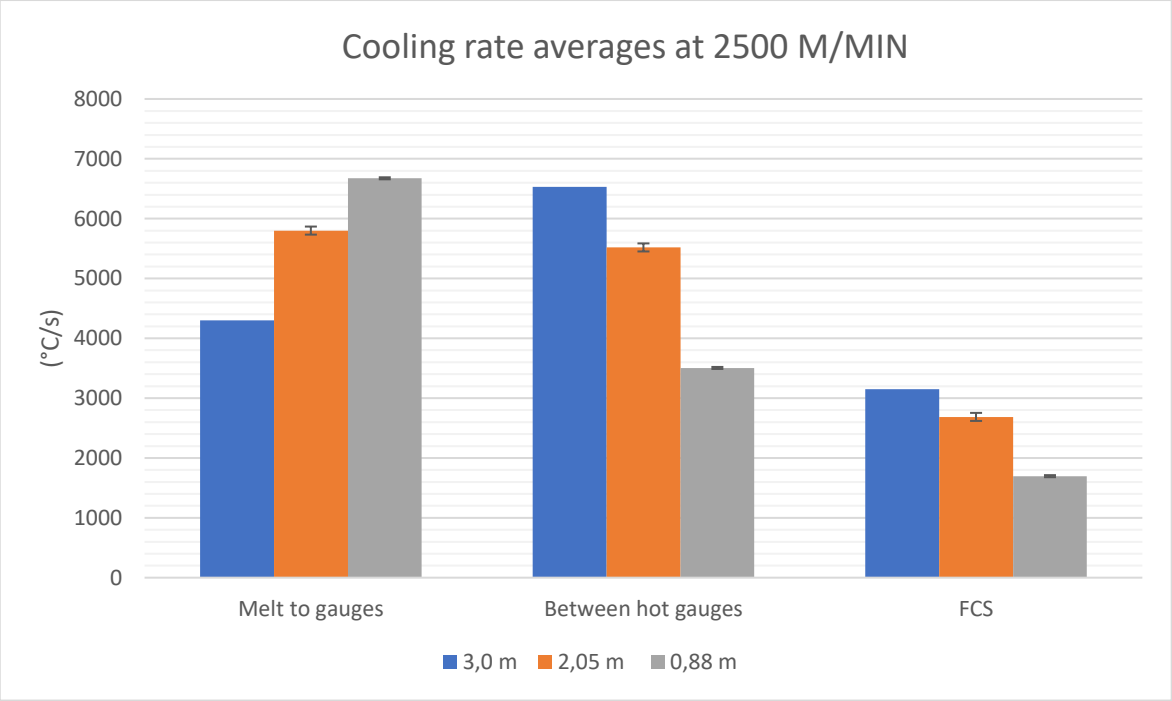

Figure 10. Comparison of extension tube lengths and their calculated cooling rate average from all draws.

If the draws D200416 and D200421 should be excluded for being anomalies with abnormal preform, we can see slightly a less steep linear projection for *ΔT1* in Figure 11. The positive

relationship between *ΔT1* and measured attenuation still remains. However, if same doubt is considered in the case of D200604 which attenuation values of over 0.190 dB/km at 1550 nm, then the positive relationship starts to be insignificant. In such case the actual nature of the relationship of the two values would need a greater number of tests to prove.

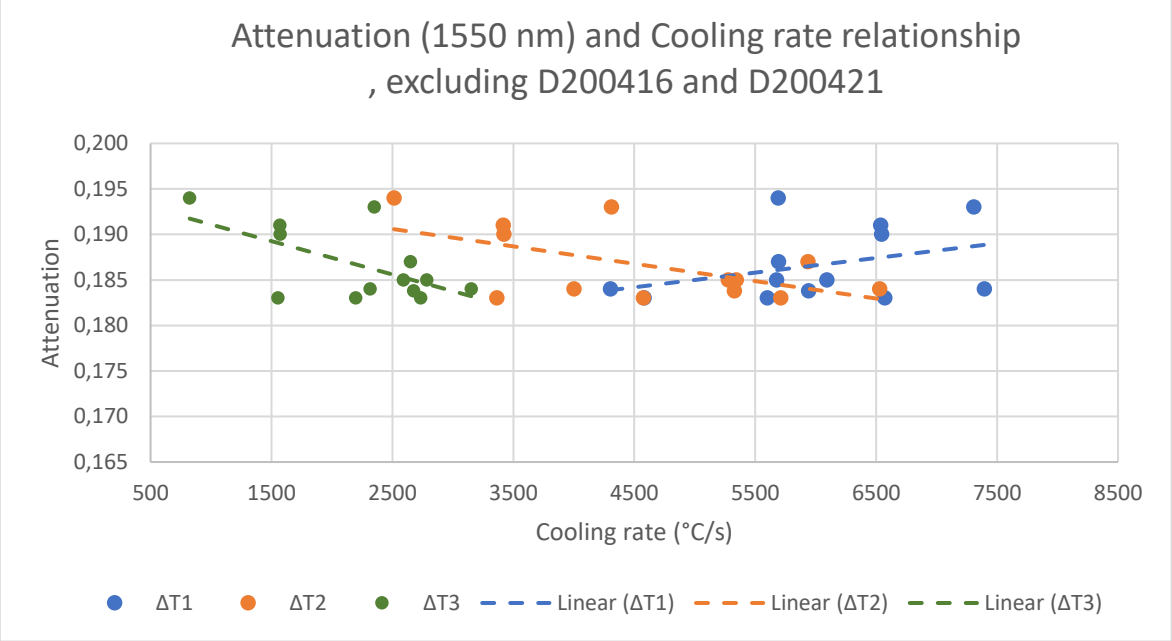

Figure 11. Plotted data of cooling rate and attenuation (at 1550 nm) values. Draws D200416 and D200421 have been excluded from this graph. Dash lines are estimated linear trendlines.

The measured data for attenuation in 1310 nm is uniform in nature with the previously discussed findings at 1550 nm. As we can see in Figure 12 the portrayed trend lines are in same orientation. However, in the 1310 nanometer wavelength the four highest attenuation values that scatter the group are all from the same draw D200604. In that draw the 0.88 meter extension tube was used for the second time. The other draw D200528 had much more common values measured as attenuation (see Table 39). With only two draws from separate preforms as data the distinction between outliers and natural scattering is not unclear. On both days the speeds tested were 2000 and 2500 m/min, the tensions were similar values around 0.70 Newtons. Even the furnace powers were comparable as both had samples measured after touchdown event. In Figure 13 we can see clearly how all trendlines have shifted if results from D200604 are excluded.

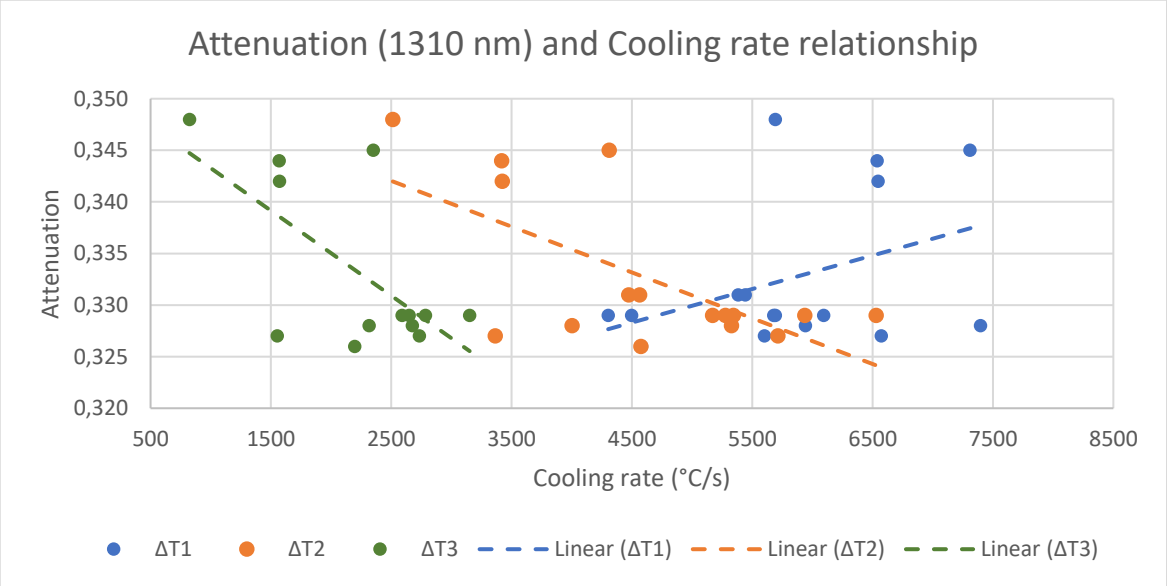

Figure 12. Plotted data of cooling rate and attenuation values at 1310 nm. Dash lines represent linear trendlines.

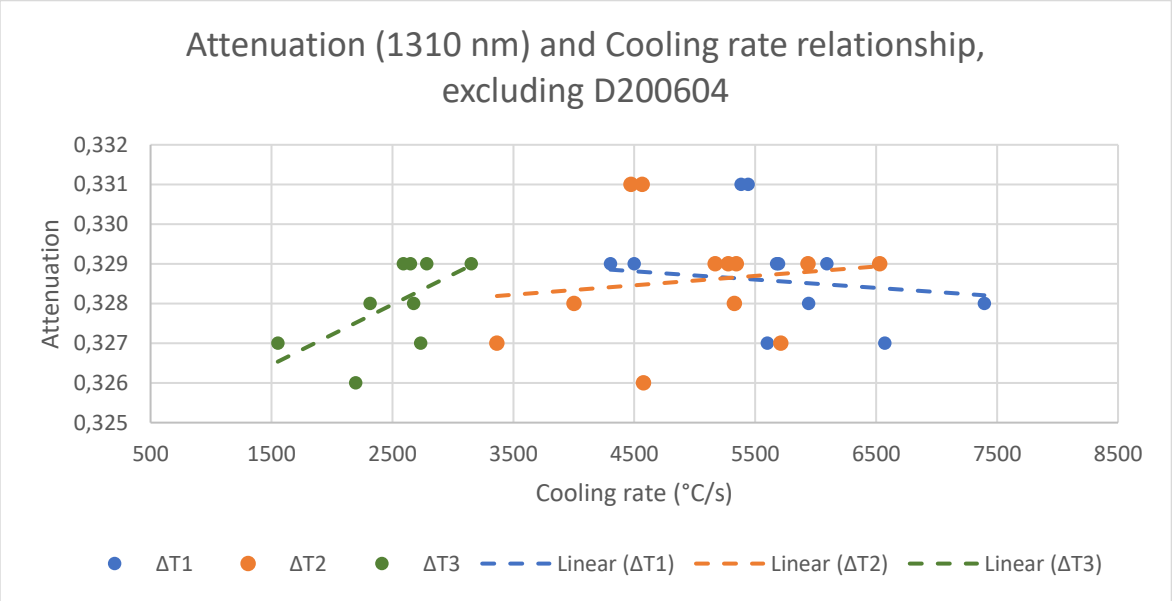

Figure 13. Plotted data of cooling rate and attenuation values at 1310 nm, but all four samples of draw D200604 were excluded from this graph.

6 DISCUSSION

During April and May, the challenges in Nextroms own preform production, as well as external influencers like SARS-CoViD-19, resulted in fewer than planned draws for this study. As a result, the final set of data was not as robust as was initially hoped for. In addition to the amount of draws to take samples from, the length and consistent quality of preform would have aided in the quality of final results. Longer preforms would have made it possible to test all three extension tube lengths with a singular preform. Thus, eliminating variables that can be experienced from preform to preform. Consistent and proven quality of preforms that all have the same origin would have also mitigated the differences that were come from changing the preform. As a sum the scattering of the results and therefore the dependability of results could be improved.

The main concern with this research and its results is the amount, dependability and repeatability of the test draws. As Nextrom Oy is an equipment manufacturer but not a optical fiber producer, the quantity of tests will stay very low. This will always result in unwanted changes to the process that degrade the dependability of the experiments. An ideal surrounding would be a fixed preform type in large production volume that gives opportunity to quantify differences between preforms and to collect many samples from each singular preform. Much of the problems faced were also exaggerated by a deadline that was not extendable due to decisions made by vice president of the university.

The deduction of attenuation in the two draws D200416-1-C and D200421 cannot be counted on as legitimate evidence without a larger sample size. Also, it is unfortunate that the greater changes to certain attenuation and other values can become from the preforms that are of secondary quality. Most of the preforms used for the research were received as cooperative gifts or for low sum as they are not up to the preform manufacturers high standards. As a consequence, the information about the manufacturing data of the preform cannot be easily confirmed to rule out preform as a variable. In ideal situation the R&D work with Nextrom preform manufacturing equipment would be on a constant high standard and providing a

steady supply of preforms to test with. Each preform would be inside Nextroms own database for quality control.

Experiments and measuring focused on ease of operation and repeatability. Working with only single SIKORA hot fiber temperature measurement gauge meant that the position had to be changed by hand during the draw in order to record the fiber temperature at different heights. This limited the amount of positions possible for measuring and also completely eliminated any unplanned passive data collection. Unless a conscious effort was made during another R&D test, to climb the draw tower and change the gauge position, the data would not be collected. The chosen three measurement positions were based on free fiber length. Shorter 0.88 m extension tube would have enabled measurements to be taken two meters higher than the actual highest point, but this data would not have been comparable to any numbers recorded with the longer quartz tubes. Furthermore, the length of existing cables meant that such high measurements would have needed a sizeable hardware change in the form of re-routing a longer set of cables. All in all, the biggest improvement would have been an additional hot SIKORA gauge to collect the necessary data continuously. If such improvements will happen in the future, it would enable passive data collection.

7 CONCLUSIONS

As was concluded before and what was evident in the Figures 8 and 11, the formed trendlines seem to suggest that the attenuation improves as the cooling rate gets smaller. This was most evident in the 1550 nanometer wavelength measurements of the attenuation that showed improvement even after excluding a set of potential outliers. With 1310 nm wavelength the data was more scattered and adjusting analyzed data group by removing a single draw day D200604 resulted in almost complete leveling of the trendline. This implies that the set of data collected too small to be significant.

The results of the done experiments must be considered with healthy skepticism. As mentioned earlier the amount of data collected was not large enough to state anything conclusive. Efforts can easily be made to correct most of the faults. The preforms were perhaps the largest variability in this research. Their quantity in numbers, their drawable length and their uniformity were all detrimental to the dependability of the results. Without deadline restrictions the continuous analysis will improve on each of these weaknesses, as we can collect further data from future preforms that have both longer length and have a higher degree of quality. Spring of 2020 has been a challenge for many reasons that are out of our control and its economic consequences perhaps even affected these experiments indirectly.

As continuation to the existing data collection the existing singular temperature measurement gauge can be utilized for passive data collection. Mapping the existing temperature readings from a constant gauge position will enable the cooling rate to be tracked along with the offline measurements with the Photon Kinetics fiber analysis devices. At the time of finishing this thesis, an improvement had been already made to automatically store all fiber measurements with the PK-devices into a database. From now onwards it is possible to retroactively track cooling rates and their effects on measured fiber properties. This will prove useful especially when busy work schedule will make it difficult to have attention for an expanding number of tasks, but the evidence can be analyzed at a later time.

REFERENCES

Azadeh, M. Fiber Optics Engineering. 2009. USA. Springer. 378 pages.

Bukshtab, M. 2019. Photometry, Radiometry, and Measurements of Optical Losses. United Kingdom. Springer. 807 pages.

Fiber Onda online data-base, [Referred to 14.11.2017], "Single-Mode vs. Multi-Mode Fiber Optic Cable", available: http://fiberonda.com/single-mode-vs-multi-mode-fiber-optic-cable/

Helk, T. 2020. SIKORA Service Engineer, private correspondence. Germany. 1 page.

IEEE online library. 2017. Available: https://ieeexplore.ieee.org/document/7937161

Kim, D.-L. & Tomozawa, M. 2000. Fictive temperature of silica glass optical fibers – re-examination. USA. Elsevier. 7 pages.

Lancry, M., Regnier, E. & Poumellac, B. 2012. Fictive temperature in silica-based glasses and its application to optical fiber manufacturing. France. Progress in Materials Science No 57. pages 63-94.

Mauro, J., Loucks, R. & Gupta, P. 2009. Fictive Temperature and the Glassy State. USA. Journal of The American Ceramic Society. 12 pages.

Mitschke, F. 2016. Fiber optics. Germany. Springer-Verlag. 350 pages.

Neumann, E.-G. 1988. Single-mode fibers: Fundamentals. Germany. Springer-Verlag. 542 pages.

Ohashi, M., Shiraki, K. & Tajima, K. 1992. Journal of Lightwave Technology, VOL. 10, No. 5. 539-543 pages.

Reinhold, N. 2010. Essentials of Modern Optical Fiber communication. Germany. Springer-Verlag. 289 pages.

Rosendahl Nextrom Oy. 2018. OFC 20 Technical Data sheet. [Referred to 13.5.2020]. Available: http://www.rosendahlnextrom.com/fiber-optics/file/2018/03/OFC-20_Fiber-Draw-Tower.pdf

SIKORA webpage. Fiber Series 6000. [Referred to 19.4.2020]. Available: https://sikora.net/en/products/fiberseries6000/

Telecommunication Standardization Sector of ITU. 2017. ITU-T G.652. [Referred to 17.5.2020]. 28 pages. Available: https://www.itu.int/rec/T-REC-G.652-201611-I/en

Telecommunication Standardization Sector of ITU. 2014. ITU-T G.654. [Referred to 19.4.2020]. 24 pages. Available: https://www.itu.int/rec/T-REC-G.654-201611-I/en

Ter-Mikirtychev, V. 2014. Fundamentals of Fiber Lasers and Fiber. Switzerland. Springer. 269 pages.

Volotinen, T., Konkarikoski, A., Arvidsson, B. and Ericsson, K. 2003. Impact of silica glass structure on transmission properties of Ge-doped single-mode fibers. Sweden. OFCON AB. 13 pages.